GENERAL ATOMIC

GA-A14040
UC-77

FATIGUE LIFE EVALUATION OF CONNECTIONS BETWEEN THE HTGR THERMAL BARRIER ATTACHMENT FIXTURES AND THE PCRV LINER

by
S. RODKIN and G. WONACOTT

Prepared under
Contract EY-76-C-03-0167
Project Agreement No. 50
for the San Francisco Operations Office
U.S. Energy Research and Development Administration

GENERAL ATOMIC PROJECT 3218

DATE PUBLISHED: JANUARY 1977

ABSTRACT

The results of a development program to evaluate the fatigue life of the welded stud connections between the HTGR thermal barrier attachment fixtures and the prestressed concrete reactor vessel (PCRV) liner are presented.

The corrective actions taken to remedy the problems disclosed by this program are also described.

CONTENTS

ABSTRACT iii

1. SUMMARY 1-1

2. THERMAL BARRIER DESCRIPTION 2-1

3. CONCLUSIONS 3-1

4. CORRECTIVE ACTION 4-1

5. LOADS 5-1

5.1. Operational Load Sources 5-1

5.1.1. Primary Steady-State Mechanical Load 5-1

5.1.2. Primary High Cycle Fatigue Load 5-1

5.1.3. Secondary Thermal Loads 5-1

5.1.4. Secondary Steady-State Mechanical Load 5-2

5.2. Operational Load Cycles 5-2

6. TEST PROGRAM 6-1

6.1. General 6-1

6.2. Test Subcontractor 6-1

6.3. Test Equipment 6-1

6.4. Test Items 6-2

6.4.1. Welded Studs and Base Plates 6-2

6.4.2. Central Attachment Fixtures and Mid-Edge Retainers 6-3

7. TEST PROCEDURE 7-1

7.1. Test Item Setup. 7-1

7.2. Test Machine Operation 7-2

7.3. Special Test Procedure 7-2

8. RESULTS OF FATIGUE TESTS 8-1

9. DISCUSSION 9-1

9.1. General 9-1

9.2. Chatter 9-1

9.3. Superposition of Stud Stresses 9-3

9.4. Attachment Fixture Failures 9-4
9.5. Metallurgical Examination 9-4
10. REFERENCES 10-1

FIGURES

1. (a) Typical thermal barrier cover plate. 2-3
1. (b) Typical thermal barrier section. 2-4
2. Typical thermal barrier attachment fixture 2-5
3. Central attachment fixture 4-3
4. Mid-edge retainer 4-4
5. Overall view of test equipment set up for applying transverse stud loads through a Class B MER 6-4
6. Class A CAF set up for application of axial stud loads . . . 6-5
7. Class B MER being prepared for axial load application 6-6
8. CAF studs after quasi-static application of ultimate load . . 6-7
9. Stud numbering system and orientation of transverse load . . 7-4
10. Results of axial input CAF cyclic failure tests 8-6
11. Results of transverse input CAF cyclic failure tests 8-7
12. Results of axial input MER cyclic failure tests 8-8
13. Results of transverse input MER cyclic failure tests 8-9
14. Soderberg diagram showing reciprocal relationship between the steady-state and alternating stress amplitudes 9-6
15. SEM photomicrographs showing the stud specimen surface believed to be the fatigue initiation site. 9-7
16. SEM photomicrographs showing the shear rupture area of the stud specimen 9-8
17. (a) Microstructure of cross-sectional area perpendicular to fatigue initiation site in the specimen. 9-9
17. (b) Microstructure of cross-sectional area perpendicular to fatigue area in the specimen 9-10
17. (c) Microstructure of cross-sectional area perpendicular to shear rupture area in the specimen 9-10
18. Typical microstructures at (a) the crest and (b) the root in the thread area for an untested 1/2-in. stud. 9-11

TABLES

1. Operational load sources 5-3
2. Fatigue test results - transverse loading 8-3
3. Fatigue test results - axial loading 8-5

1. SUMMARY

The objective of the test program described herein was to evaluate the fatigue life adequacy of the welded stud connections between the thermal barrier attachment fixtures and the PCRV liner in the HTGR. The fatigue life of the welded studs is an important design consideration for the following reasons: (1) cyclic loading is induced in the studs by normal reactor thermal cycling; and (2) the postulated occurrence of stick-slip, or chatter, at the thermal barrier cover plate/attachment fixture interface during reactor thermal cycling has a multiplying effect on the number of load cycles required of the studs.

The test loads were applied to the studs through typical thermal barrier attachment fittings so as to accurately reproduce the complex stud loadings generated by the geometry of the fittings.

Three problem areas were discovered:

1. The attachment fittings themselves failed under certain loading conditions. These failures were due to poor quality castings and to local stress concentrations. The use of castings has been suspended, and the stress concentrations have been eliminated by subsequent redesign.

2. The geometry of the attachment fixture flange induced combined steady-state stresses in the studs such that the design fatigue life could not be demonstrated. Owing to this problem, redesign of the attachment fixtures was performed. Retesting is planned to evaluate stud fatigue life using the redesigned attachment fixtures.

3. The contribution of chatter to the fatigue life requirement must be evaluated. Planning for this effort is currently in progress.

2. THERMAL BARRIER DESCRIPTION

The functions of the thermal barrier are (1) to control the temperature levels and gradients in the PCRV liner and the PCRV in conjunction with the liner cooling system and (2) to minimize heat losses from the primary coolant system. In zones where the temperature does not exceed 1700°F, these functions are provided by layers of fibrous insulation blankets which are compressed against the PCRV liner by cover plates [see Figs. 1(a), 1(b), and 2*]. Insulation blankets of varying thickness and composition are used, dpending upon the hot-side temperature and other factors. In zones where the maximum operating temperature is 750°F, the insulation has been designated Class A insulation. Class B insulation is used in zones where the maximum temperature does not exceed 1700°F. (Class C insulation is used in still higher temperature zones. The attachment method for Class C insulation is not similar to that for Class A and B and was not included in this development program.)

The Class A and Class B insulation cover plates are held in place by attachment fixtures which pass through the insulation and are fastened by threaded studs welded to the liner. Seal sheets are provided to bridge the gaps between cover plates and retard permeation of the insulation blankets by the hot gas.

An attachment fixture, called the central attachment fixture (CAF), is located at the center of each cover plate. Four additional fixtures, one at the mid-point of each edge of each cover plate, are used to control deflection of the edges. These fixtures, called mid-edge retainers (MERs), are shared by adjacent cover plates. Each CAF is fastened to the liner by 1⁄2-in.-diameter welded studs. Each MER is fastened by 3/8-in.-diameter welded studs.

---

*Figures and tables appear at the end of each section.

The CAFs and MERs employed in support of the Class B insulation are longer than those used for Class A owing to the greater insulation thickness. Hastelloy X is required for the Class B CAFs and MERs to meet the temperature requirement. Castings of Hastelloy X were investigated as a cost-saving alternative to forging and machining. Carbon steel (AISI 1020) is used for the Class A CAFs and MERs. Identical stud material and stud welding procedures are used for Class A and Class B attachments.

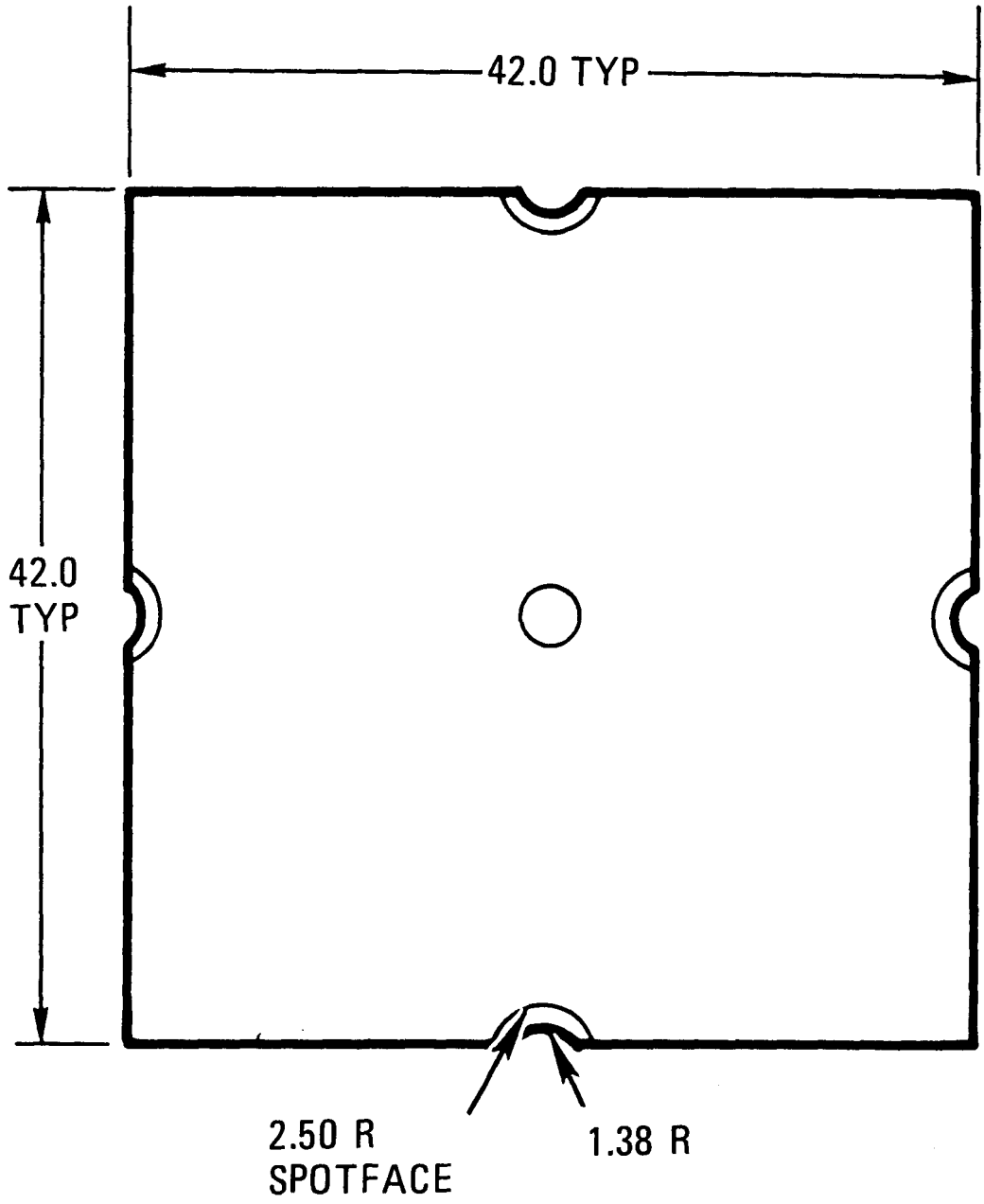

Fig. 1(a). Typical thermal barrier cover plate

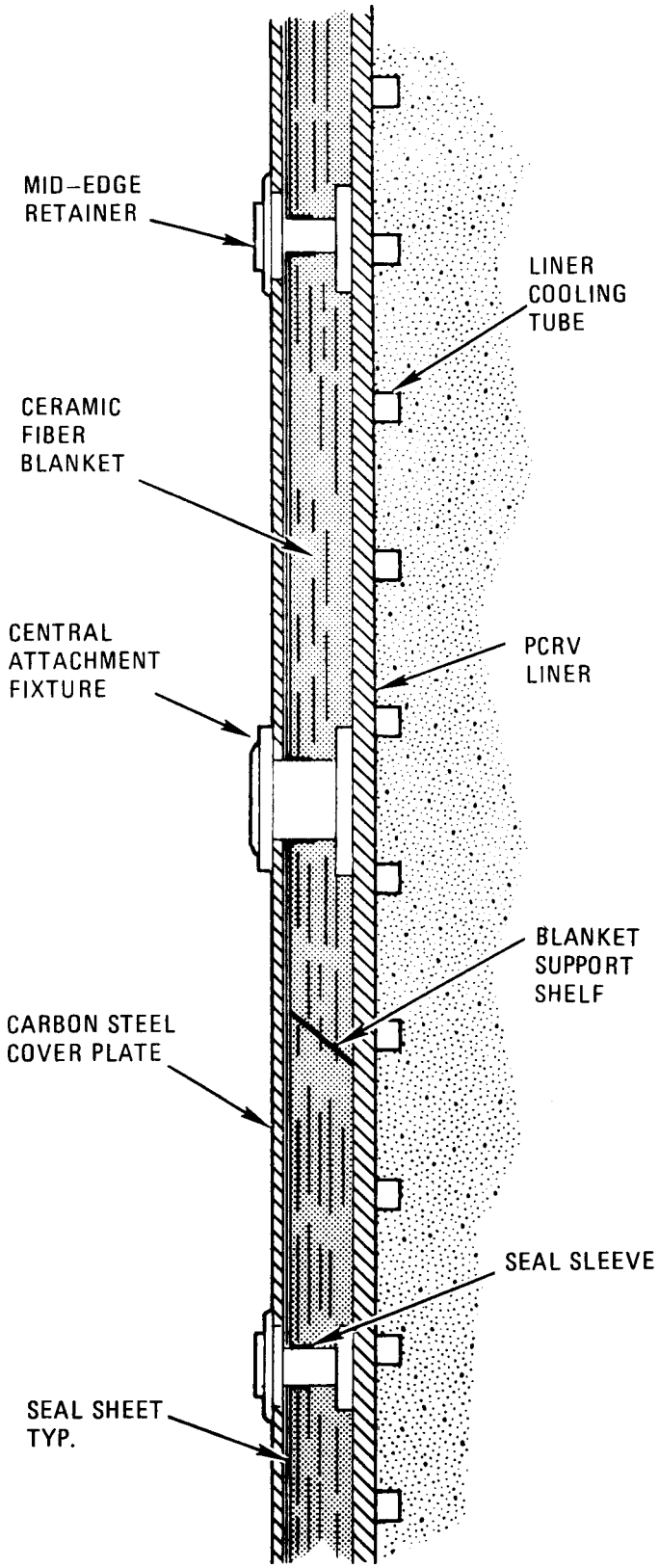

Fig. 1(b). Typical thermal barrier section

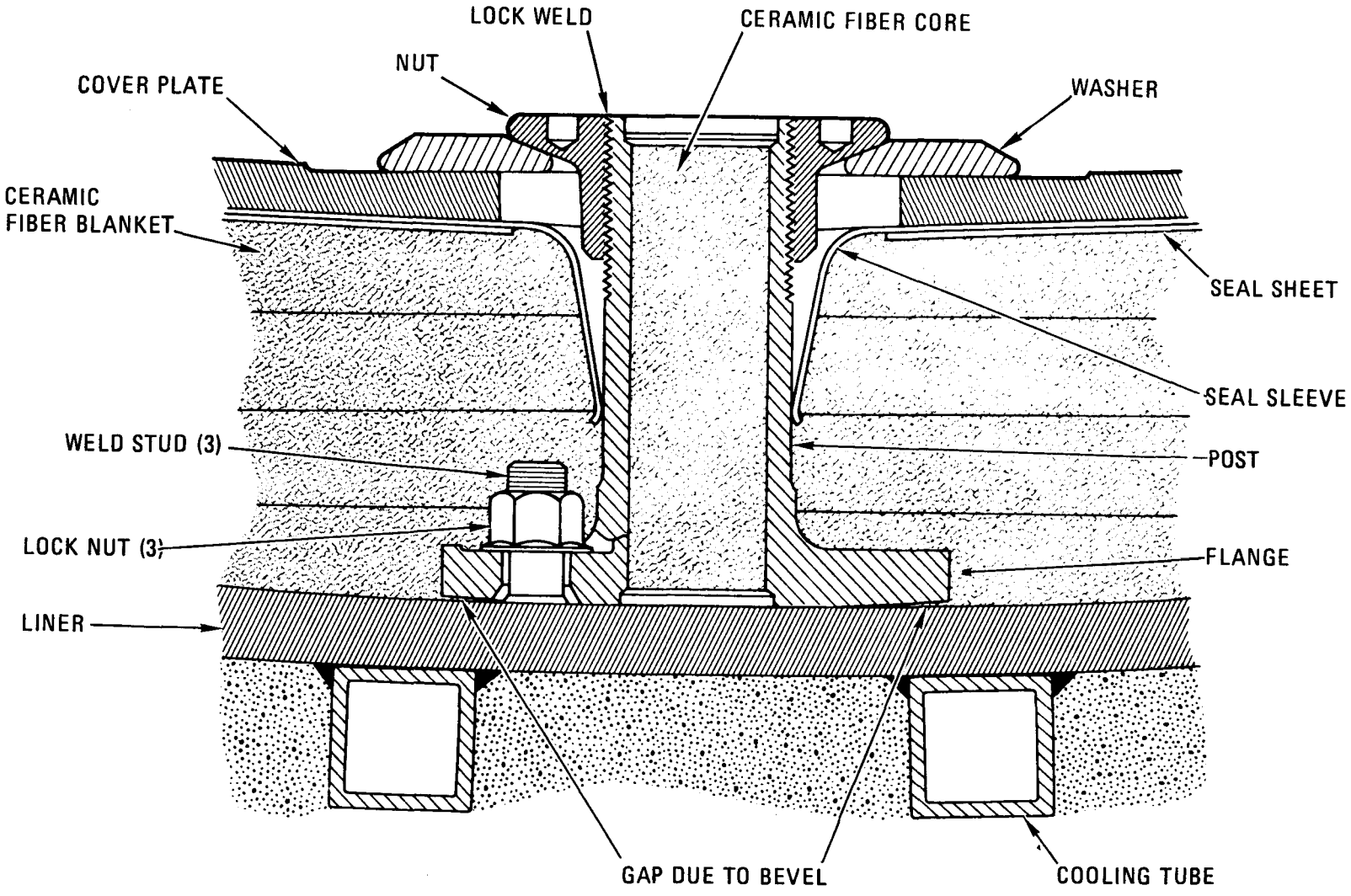

Fig. 2. Typical thermal barrier attachment fixture (Class A and Class B)

3. CONCLUSIONS

The significant conclusions which can be drawn from this development program are as follows:

1. The welded stud connections between the attachment fixtures and the PCRV liner provided inadequate safety margins with respect to the postulated fatigue life requirements.

2. Experimental evaluation of the fatigue life requirements was found to be necessary.

3. The attachment fixture design was inadequate for the postulated cyclic load environment.

4. The grain structure of the Hastelloy X castings was poorly controlled.

The inadequate fatigue life of the welded studs was due primarily to the large steady-state bending and axial stresses induced during pre-loading. These steady-state stresses significantly reduced the fatigue capability of the studs.

The postulated occurrence of chatter at the cover plate/attachment fixture interface during reactor temperature changes imposes severe fatigue life requirements on all portions of the attachment fixture, including the studs by which each fixture is secured to the PCRV liner. The fatigue life requirements were established analytically using conservative methods of chatter amplitude and frequency prediction. The chatter parameters should be evaluated experimentally.

The attachment fixture fatigue failures, both in the external threads of the cylindrical section and in the spot face of the base flange, were caused by amplification of the stresses by stress risers. In general, the failures occurred at load magnitudes greater than the current design loads. However, improvement in the problem areas has been achieved through redesign.

4. CORRECTIVE ACTION

Experimental determination of chatter parameters is currently scheduled for FY-77 and FY-78 (Ref. 1). Planning for reevaluation of stud fatigue life using the redesigned attachment fixtures is under way.

The attachment fixtures have been redesigned to minimize the stress concentrations and to reduce the stresses in the studs due to pre-loading. Stud pre-load has been reduced from 540 to 260 in.-lb for the 1/2-in. CAF studs and from 210 to 160 in.-lb for the 3/8-in. MER studs. The three-stud triangular flange has been replaced with a four-stud rectangular flange having greater contact area to improve the fixture stability. This results in more equal load distribution among the studs and lower axial stresses. The flange thickness has been increased and the beveled portion shortened, resulting in greater flange stiffness and reduced bending stress in the studs.

The design changes in the fixtures as a result of this development program are summarized below. Unless noted, the changes apply to both the CAFs and MERs.

1. Increased the wall thickness in the cylindrical section.

2. Increased the thickness of the flange.

3. Eliminated the spot face at the stud hole in the flange.

4. Shortened the external thread at the cover plate end (MER only).

5. Replaced the triangular flange with a rectangular one.

6. Increased the number of studs from three to four.

7. Reduced the length of the non-contacting or beveled section of the flange.

8. Suspended the use of cast Hastelloy X.

Figure 3 shows the CAF before and after the redesign. Figure 4 shows the MER before and after the redesign.

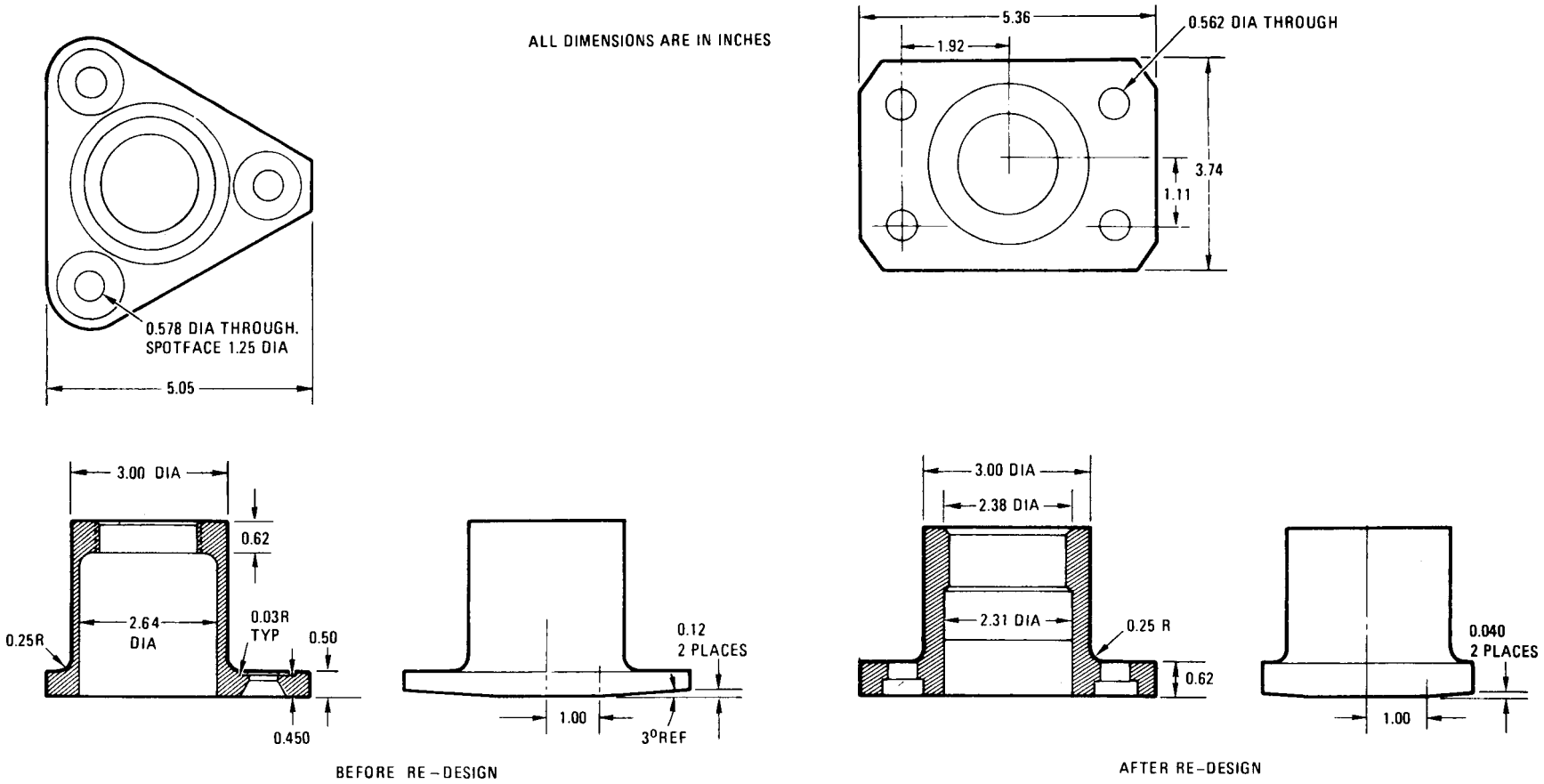

Fig. 3. Central attachment fixture

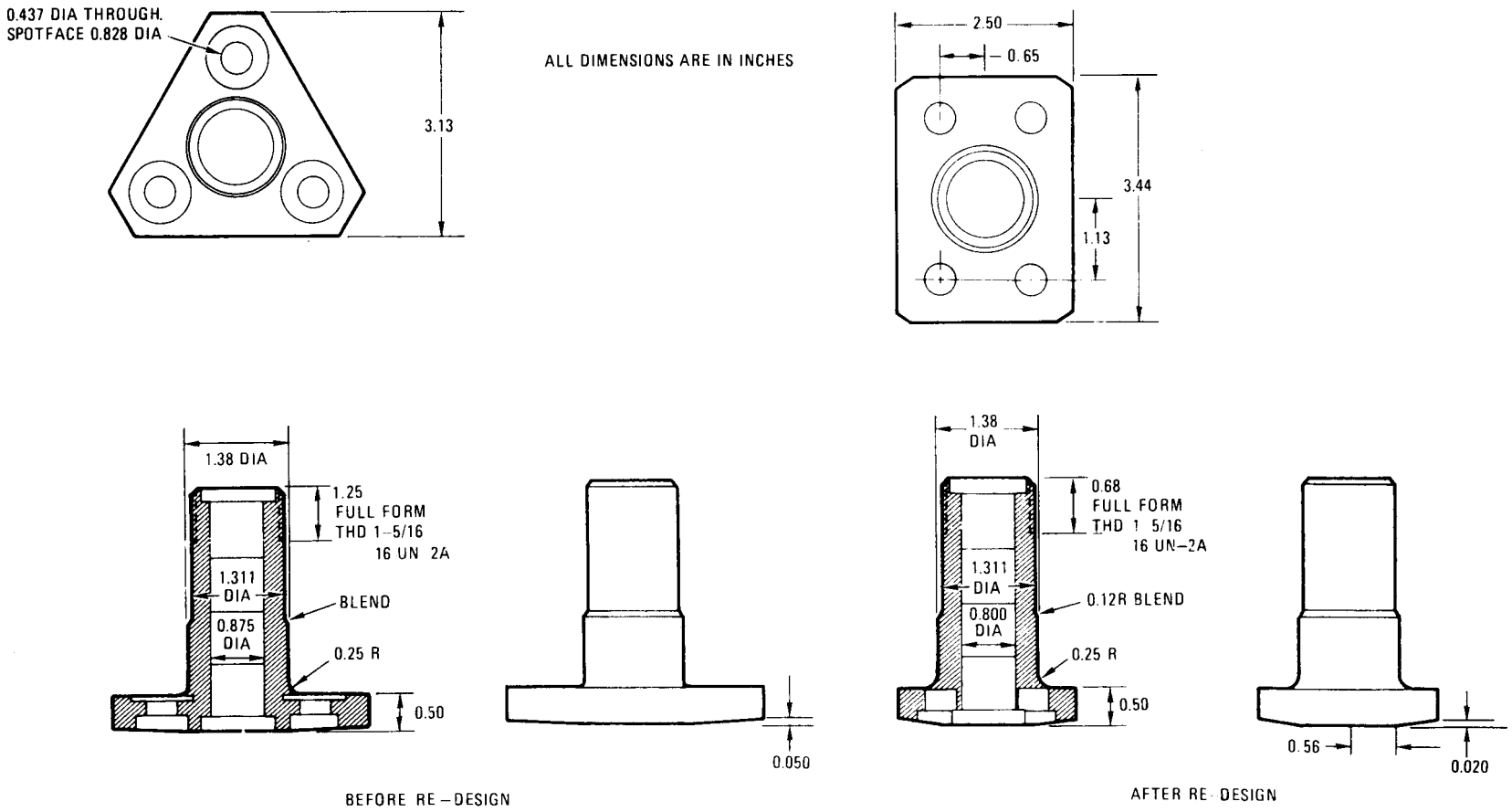

Fig. 4. Mid-edge retainer

5. LOADS

5.1. OPERATIONAL LOAD SOURCES

The loads applied to the attachment fixtures, and hence to the welded studs, are both steady state and cyclic. These loads arise from mechanical means, from axial thermal gradients, from cover plate thermal expansion, and from installation pre-load torque, as described below and shown in Table 1.

5.1.1. Primary Steady-State Mechanical Load

The primary (Ref. 2) steady-state mechanical load is due to the reaction to the fibrous insulation pressure. This is an axial load in the attachment fixtures. It translates into tensile stud stresses, and in some of the studs a bending component is also induced. The reason for the bending component is discussed in Section 9.

5.1.2. Primary High Cycle Fatigue Load

The primary high cycle fatigue load is a mechanical load arising from cover plate thermal expansion and contraction. It translates into tensile and bending stresses in the studs. The postulated existence of chatter produces a high cycle fatigue loading condition.

5.1.3. Secondary Thermal Loads

Secondary (Ref. 2) loads arise from the axial thermal gradient in the attachment fixtures. These are due to the tendency of the hot end to expand diametrically more than the cold end, to the large stiffness of the flange relative to the cylindrical section, and to the large stiffness and

low temperature of the liner relative to the attachment fixture flange. These conditions translate into low cycle bending and shear stresses in the studs.

5.1.4. Secondary Steady-State Mechanical Load

Another secondary steady-state mechanical load on the studs arises from the installation pre-load or the application of torque to the nuts securing the attachment fixture flange against the liner. This load translates into tensile and bending stresses in the studs. The bending stresses are due to flexure of the attachment fixture flange. This load is discussed in Section 9.

5.2. OPERATIONAL LOAD CYCLES

The high cycle fatigue loading is due to cover plate thermal expansion and contraction associated with reactor thermal cycles. Table 1 indicates that a total of 22,400 reactor thermal cycles will occur over the life of the plant. Intermittent motion at the cover plate/attachment fixture interface, called stick-slip or chatter, was postulated to significantly increase the number of stress cycles occurring at the cover plate end of the CAFs and MERs for each reactor thermal cycle. The existence of the chattering phenomenon is well documented (Refs. 3-5). However, the load range and the number of chattering cycles produced are highly dependent upon the particular dynamic system. The parameters affecting the chattering response are the spring rates and masses of the parts, external vibration, temperature, friction coefficients of the sliding surfaces, sliding rates, normal forces between surfaces, and, in this application, impurities in the gas coolant and curvature of the cover plates.

Analysis indicates that chattering may cause an increase in the fatigue life requirement to 10^8 cycles. (See Section 9.2.)

TABLE 1
OPERATIONAL LOAD SOURCES

Load Source	Load Classification	Type of Stud Stress Induced	Attachment Fixture Stress Cycles
Insulation pressure	Primary steady-state	Tensile, bending	--
Cover plate thermal expansion	Primary high cycle	Tensile, bending	10^8
Attachment fixture axial thermal gradient	Secondary low cycle	Bending, shear	22,400
Lock nut installation torque	Secondary steady-state	Tensile, bending	--

Note: The total number of reactor design thermal cycles due to start-up, operational and accident transients, and shutdown is 22,400 (Ref. 6).

6. TEST PROGRAM

6.1. GENERAL

The test program was designed to evaluate the room temperature fatigue life of the studs under separate axial and transverse loading. Curves of applied load versus cycles to failure were generated for each of the two stud sizes and for each load condition.

No attempt was made to test specimens up to the high number of cycles (10^8) postulated by the chatter theory, since this would have required an extremely long and costly program. For example, tests to 10^7 cycles required 4 to 6 days of continuous test machine time, depending upon the achievable cyclic rate. Testing up to 10^8 cycles would have required 40 to 60 days per test specimen; consequently, the plan was to generate as much of the curves of fatigue failure load versus number of cycles as possible within reasonable cost and time constraints and to extrapolate the results to 10^8 cycles. This plan was to be supplemented by an experimental investigation of the validity of the chatter assumptions.

6.2. TEST SUBCONTRACTOR

The test subcontractor was the Materials and Processes Department, Convair Division, General Dynamics Corporation. All testing was performed at the subcontractor's San Diego, California plant.

6.3. TEST EQUIPMENT

All tests were run on a 50,000-lb MTS Systems Corporation closed loop test machine. The supporting fixturing was supplied by General Atomic.

Figure 5 shows an overall view of the test equipment set up for applying transverse stud loads through a Class B MER. Figure 6 shows a Class A CAF set up for application of axial stud loads. Figure 7 shows a Class B MER being prepared for axial load application, and Fig. 8 shows the CAF studs after quasi-static application of the ultimate load.

As shown in Figs. 6 and 7, for axial loading the base or liner plates were bolted to the lower (movable) head of the test machine. Load was applied to the welded studs through the CAF or MER, which were attached to the upper (fixed) head of the test machine by an adapter and a series of links. The links were used to prevent bending loads from being induced into the CAF or MER. For transverse loading, the right-angle fixture was used to support the base plate as shown in Fig. 5.

6.4. TEST ITEMS

6.4.1. Welded Studs and Base Plates

The welded studs were made from mild carbon steel. They were supplied by Nelson Stud Welding Company, a Division of Gregory Industries Inc., Lorain, Ohio. The studs were welded to the base plates by Nelson Stud Welding Company using a semiautomatic welding procedure (Ref. 7). The weld configuration can be seen in Fig. 8. The CAF utilized three 1/2-in.-diameter, 13 threads to the inch studs, and the MER utilized three 3/8-in.-diameter, 16 threads to the inch studs.

The base or liner plates were supplied by Pittsburgh Des Moines Steel Company. The material was SA 537 steel, which is the material used in the PCRV liner. The plates were approximately 8 in. by 10 in. by 1 in. thick and were nominally flat.

The base plates are shown in Figs. 6 and 7 (immediately behind the 6-in. scale).

6.4.2. Central Attachment Fixtures and Mid-Edge Retainers

Typical Class A and Class B CAFs and MERs were used to transfer the loads to the studs. The Class A CAFs and MERs were made from AISI 1020 carbon steel and were machined from bar stock. The Class B CAFs and MERs were made from Hastelloy X using an investment casting procedure. All units were supplied by Decoto Aircraft Incorporated, Yakima, Washington.

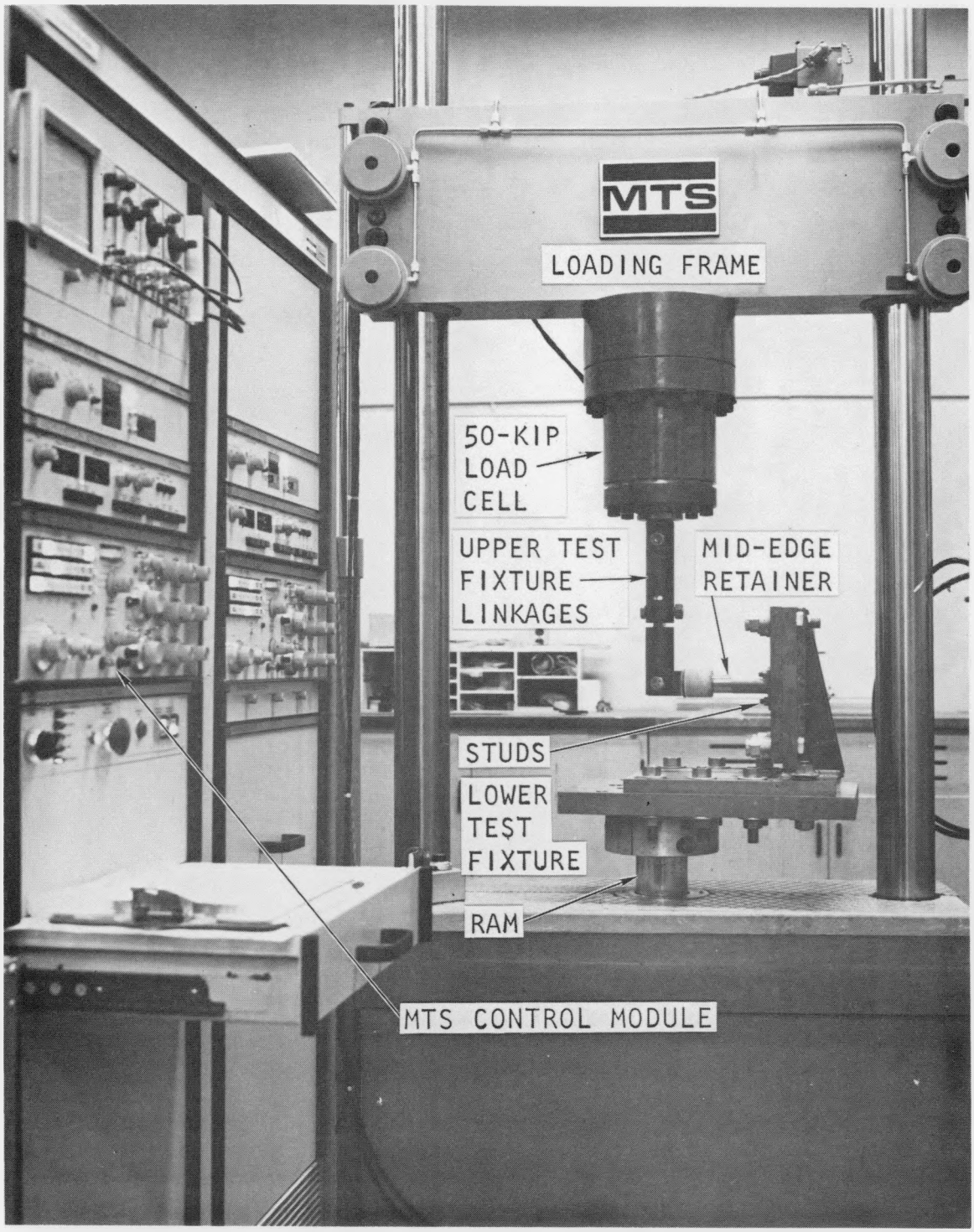

Fig. 5. Overall view of test equipment set up for applying transverse stud loads through a Class B MER

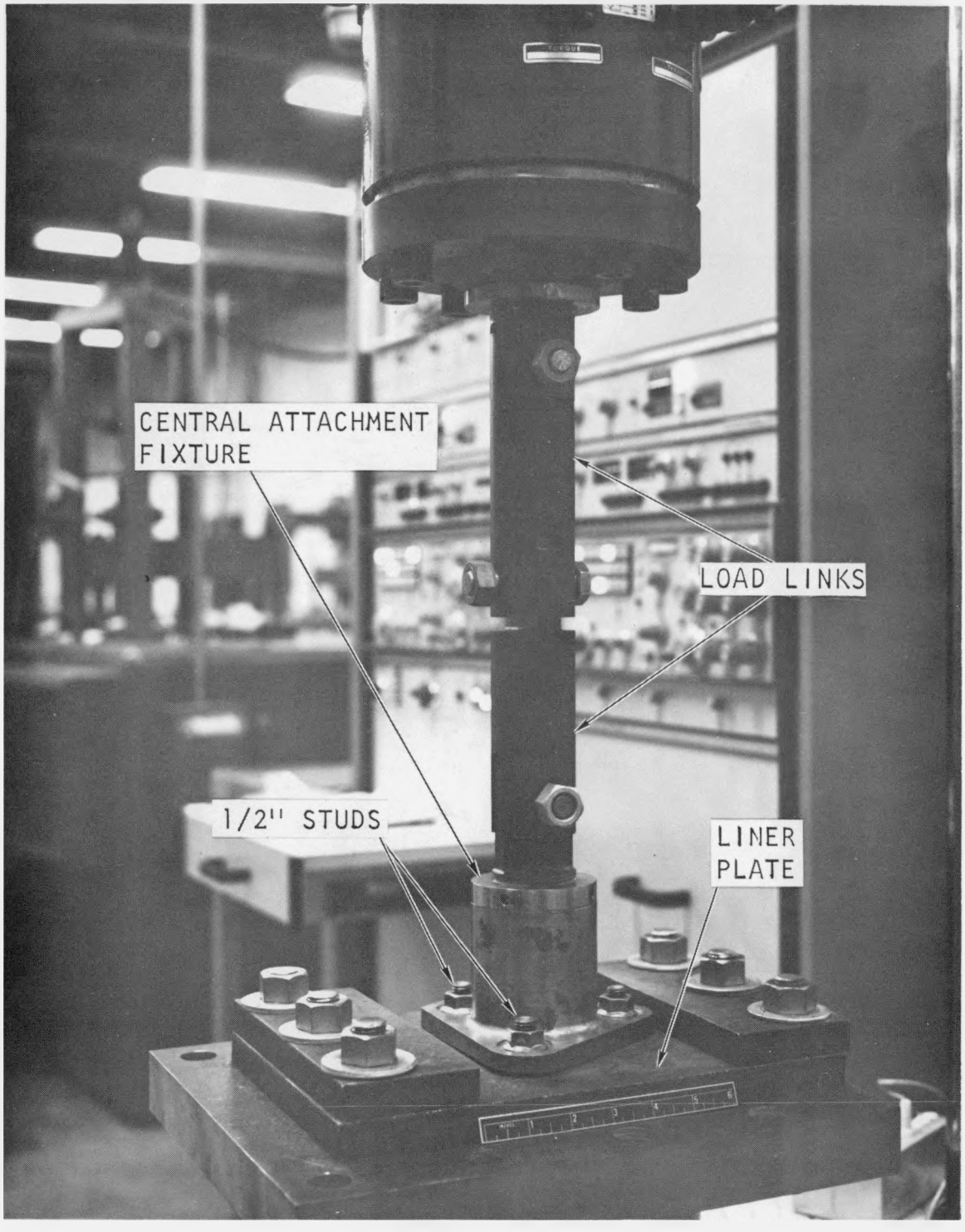

Fig. 6. Class A CAF set up for application of axial stud loads

Fig. 7. Class B MER being prepared for axial load application

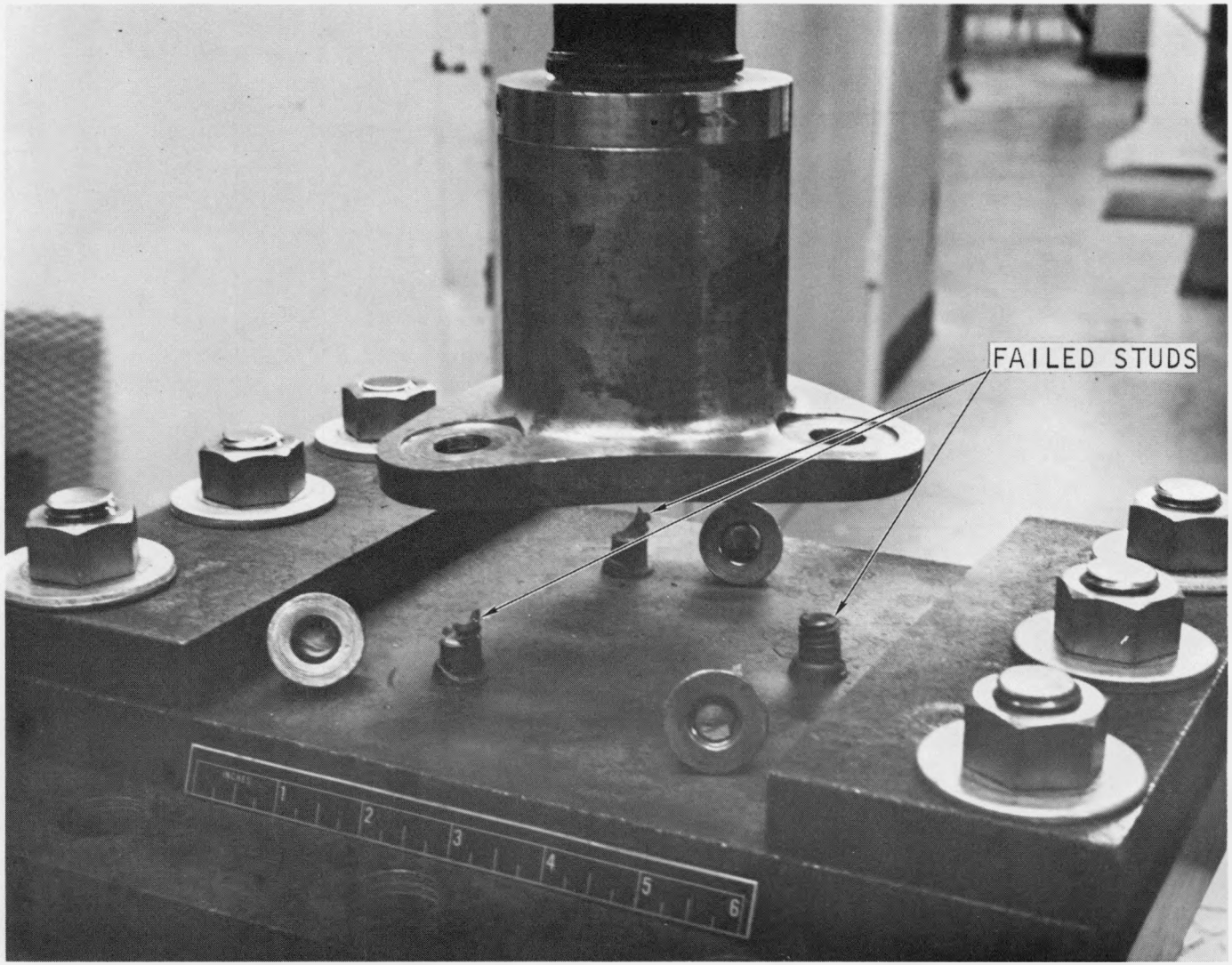

Fig. 8. CAF studs after quasi-static application of ultimate load

7. TEST PROCEDURE

7.1. TEST ITEM SETUP

After the support fixtures and base plate were properly arranged for the particular test, the attachment fixture, either a CAF or MER, was installed over the welded studs. The threaded portion of each stud was carefully lubricated with Molykote 321, which is a dry film molybdenum disulfide lubricant in a spray can. The nuts were run on and torqued according to the following sequence (see Fig. 9):

Stud	Torque
2	Finger tight
1	Finger tight
3	Finger tight
2	1/2 specified torque
1	1/2 specified torque
3	1/2 specified torque
2	Full torque*
1	Full torque
3	Full torque

The fixture was carefully aligned in the test machine to ensure that the linkage was plumb. All fixture-to-machine fasteners were torqued to the required level, and the test to failure was run. After each failure a new liner plate with new studs was installed. A new CAF or MER was also installed. The original plan was not to reuse any CAF or MER after it had been used in the load path to produce stud failure. This policy was deviated from in the later stages of the program for reasons discussed in Section 8.

Figure 9 shows the stud numbering sequence used throughout the program. It also shows the transverse loading orientation, which is a

*540 in.-lb for the 1/2-in. CAF studs; 210 in.-lb for the 3/8-in. MER studs.

representative loading case. The bevel of the lower face of the flange (CAF and MER) is indicated by the area outside the dotted lines. The bevel appears in Fig. 2 as a gap between the flange lower surface and the liner. The reason for the bevel and its effect on stud stresses are discussed in Section 9.

7.2. TEST MACHINE OPERATION

The test machine was utilized in two modes for this test: (1) quasi-static loading with x-y plots of load versus deflection, and (2) load-controlled cycling with a cycle counter and automatic shutoff at test item failure.

Determination of the quasi-static stud failure load for each configuration was necessary to establish a starting point. The quasi-static load was applied at the rate of 50,000 lb/min. The applied load versus deflection was plotted by the test equipment utilizing the signals from built-in sensors. Loading continued until failure occurred. The failure load was used as a basis for selection of the first cyclic failure load. The machine was set to apply this load automatically to the new test item at the maximum obtainable frequency, which is dependent upon the stiffness of the load path. Most of the cyclic tests were run at about 20 Hz, although in some cases it was possible to achieve a maximum of 30 Hz. The load cycle was a tension-tension cycle; i.e., the applied load varied between 100% of desired and 10% of desired ($R = 0.1 = P_{min.}/P_{max.}$). The machine was set to shut down if the load was lost, i.e., failure in the load path occurred. The load cycles were tallied by a counter in the machine.

7.3. SPECIAL TEST PROCEDURE

As the test program progressed, scattering of the data for certain loading conditions became apparent. Preliminary analysis indicated that the scatter was related to the steady-state stresses induced in the studs by the pre-load torque. More specifically, it appeared that high bending

stresses were induced in the studs as a result of deflection of the thermal barrier attachment fixture flange under the high stud pre-load. This bending stress was superimposed on the axial stress due to pre-load. In order to more clearly define the effects and interactions of the pre-load, it was necessary to obtain strain data on the studs as the pre-load torque was applied and as external transverse load was applied. A Class B CAF (Hastelloy X) and a Class B MER were used for this procedure. Three strain gages were applied to each of the three 1/2-in. CAF studs and to each of the three 3/8-in. MER studs. The pre-load torque was applied in accordance with the sequence shown in Section 7.1. The strain gage signals were read at the finger tight or zero torque, 1/2 specified torque, and full torque conditions. The strain gages were also read at each transverse load increment applied to the CAF and MER. Loading continued until stud failure occurred in each case.

The results of this special test procedure indicated that bending stresses on the order of 50 ksi maximum and axial stresses on the order of 30 ksi maximum were induced in the studs by the pre-load.

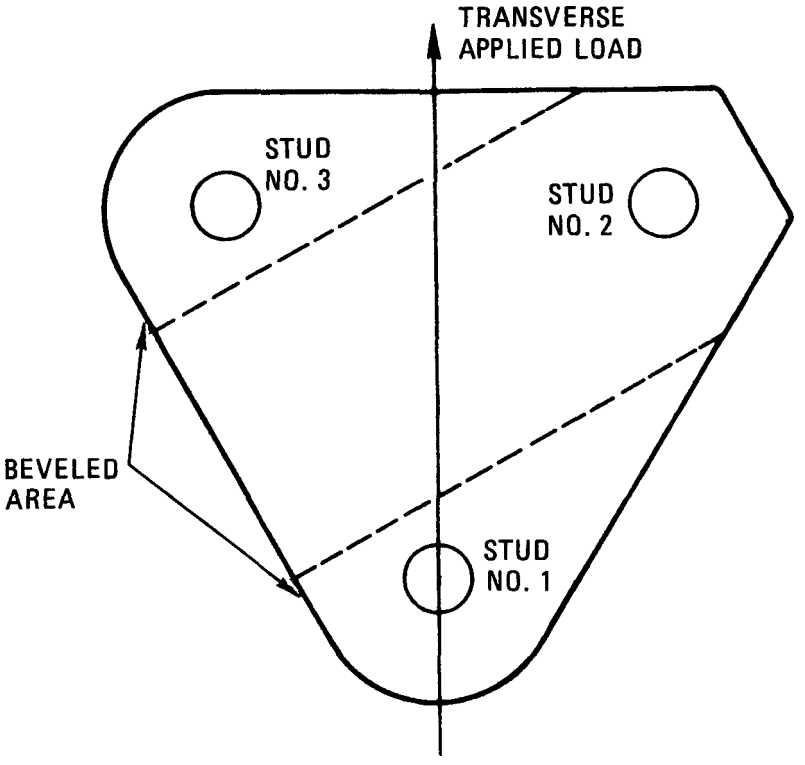

Fig. 9. Stud numbering system and orientation of transverse load (CAF and MER)

8. RESULTS OF FATIGUE TESTS

The results of this test program are shown in Tables 2 and 3 and Figs. 10 through 13. Results are discussed in Sections 8 and 9. The design values shown in the figures are developed in Ref. 8.

	Figure
CAF axial tests	10
CAF transverse tests	11
MER axial tests	12
MER transverse tests	13

The number of load cycles ranged from 1/4 (ultimate load) to 10^5 for the axial tests and to 10^7 for the transverse tests.

It was expected that the curves generated could be extrapolated to 10^8 cycles for both the 1/2-in. and the 3/8-in. studs, but this proved difficult due to data scatter and attachment fixture failures. In the case of the 3/8-in. studs under transverse loading, the MERs began to fail in the 5×10^4 cycle range. Interim fixes were made to the remaining MERs and to MERs which had previously been used to produce stud failure but had not themselves failed. Reuse of these units was a contradiction of the original test philosophy. However, this became necessary in attempting to produce stud failures in the high cycle range. Stud failures were subsequently produced out to 10^7 cycles, but the data are too limited to permit useful interpretation at 10^8 cycles.

In the case of the 1/2-in. studs, a large scatter in the data appeared in the range beyond 10^5 cycles under transverse loading. This was considered to be due to the complex stress distribution induced in the studs by the geometry of the CAF base flange in combination with the installation torque.

The failure data under axial load for 1/2-in. and 3/8-in. studs exhibit much less scatter. However, there are insufficient data to allow satisfactory extrapolation to 10^8 cycles.

TABLE 2
FATIGUE TEST RESULTS - TRANSVERSE LOADING

Specimen No.[a]	Specimen Type	Material	Loading	Quasi-Static Failure Load (lb)	Cyclic Failure Load (lb)	Cycles to Failure	Moment Arm[b]
1	CAF	CS[c]	Static	9,325			5.75
2	CAF	Hx[d]	Static	6,500			8.00
3	MER	CS	Static	2,975			5.98
4	MER	Hx	Static	2,175			8.00
5	CAF	Hx	Cyclic		3,825	550,000-800,000[e]	5.75
6	CAF	Hx	Cyclic		3,825	296,700	5.75
7[f]	CAF	Hx	Cyclic		3,484	931,200	5.74
					3,636	68,300	5.50
8	CAF	Hx	Cyclic		2,941	399,200	5.78
9	CAF	Hx	Cyclic		2,608	966,700	5.75
10	CAF	Hx	Cyclic		2,083	6,062,300	5.76
11	CAF	CS	Cyclic		7,600	779	5.78
12	CAF	CS	Cyclic		7,600	1,629	5.78
13	CAF	CS	Cyclic		6,400	3,500	5.78
14	CAF	CS	Cyclic		6,400	4,129	5.75
15	CAF	CS	Cyclic		5,000	26,648	5.75
16	CAF	CS	Cyclic		5,000	47,810	5.75
17	MER	Hx	Cyclic		1,750	4,807	8.00
18	MER	Hx	Cyclic		1,750	4,420	8.00
19	MER	Hx	Cyclic		1,500	43,898	8.05
20	MER	Hx	Cyclic		1,500	32,130	8.00
21	MER	Hx	Cyclic		300	10,015,500+	8.00
22	MER	Hx	Cyclic		600	10,000,000+	8.05
23	MER	CS	Cyclic		1,800	45,330	5.98
24	MER	CS	Cyclic		1,800	37,270	5.98
25	MER	Hx	Cyclic		2,000	110	8.00
26	MER	CS	Cyclic		2,000	27,160	6.00

TABLE 2 (Continued)

Specimen No.[a]	Specimen Type	Material	Loading	Quasi-Static Failure Load (lb)	Cyclic Failure Load (lb)	Cycles to Failure	Moment Arm[b]
27	MER	CS	Cyclic		1,500	218,000	6.00
28	MER	CS	Cyclic		1,334	355,700	6.00
49	MER	CS	Static	3,125			6.00
50	CAF	Hx	Cyclic		1,375	2,011,500	8.00
51	MER	CS	Cyclic		1,334	828,170	6.00
52	MER	CS	Cyclic		1,334	>587,420[g]	6.00
53	MER	CS	Cyclic		1,000	3,386,000	6.00
54	MER	CS	Cyclic		1,832	148,300	6.00
55	MER	CS	Cyclic		916	10,000,000+	6.00
56	CAF	CS	Cyclic		2,608	3,400,000+	5.75
57	CAF	CS	Cyclic		1,913	10,000,000+	5.75
58	CAF	CS	Cyclic		2,261	3,743,300	5.75
59	CAF	CS	Cyclic		1,913	439,800	5.75

[a] Tests were not necessarily conducted in the numerical order given.

[b] Moment arm of load measured from base plane of attachment fixture.

[c] CS = carbon steel.

[d] Hx = Hastelloy X.

[e] Machine or operator error.

[f] Repeated test.

[g] Cycle counter failed.

TABLE 3
FATIGUE TEST RESULTS - AXIAL LOADING

Specimen No.(a)	Specimen Type	Material	Loading	Quasi-Static Failure Load (lb)	Cyclic Failure Load (lb)	Cycles to Failure
29	CAF	Hx	Static	29,800		
30	MER	Hx	Static	20,400		
31	CAF	CS	Static	33,800		
32	CAF	CS	Cyclic		20,000	34,550
33	CAF	CS	Cyclic		20,000	9,670
34	CAF	CS	Cyclic		16,500	47,200
35	CAF	CS	Cyclic		16,500	168,430
36	CAF	CS	Cyclic		25,000	2,228
37	CAF	CS	Cyclic		25,000	2,364
38	CAF	CS	Cyclic		30,000	485
39	CAF	CS	Cyclic		30,000	461
40	MER	CS	Cyclic		12,500	60,640
41	MER	CS	Cyclic		15,000	6,076
42	MER	CS	Cyclic		17,500	1,499
43	MER	CS	Cyclic		19,500	50
44	MER	CS	Cyclic		19,500	118
45	MER	Hx	Cyclic		12,500	32,260
46	MER	Hx	Cyclic		12,500	94,680
47	MER	Hx	Cyclic		15,000	20,038
48	MER	Hx	Cyclic		17,500	1,864

(a) Tests were not necessarily conducted in the numerical order given.

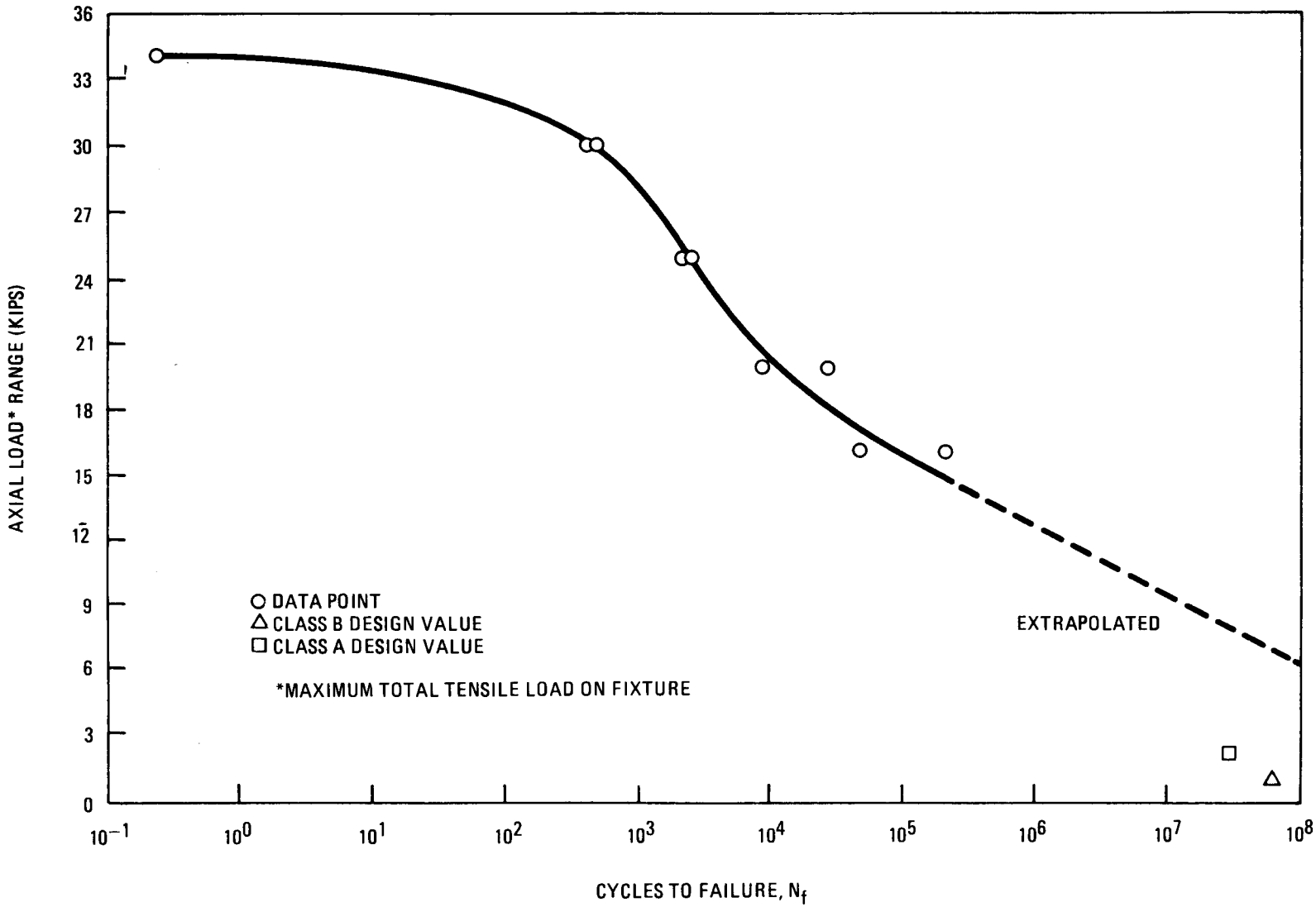

Fig. 10. Results of axial input CAF cyclic failure tests

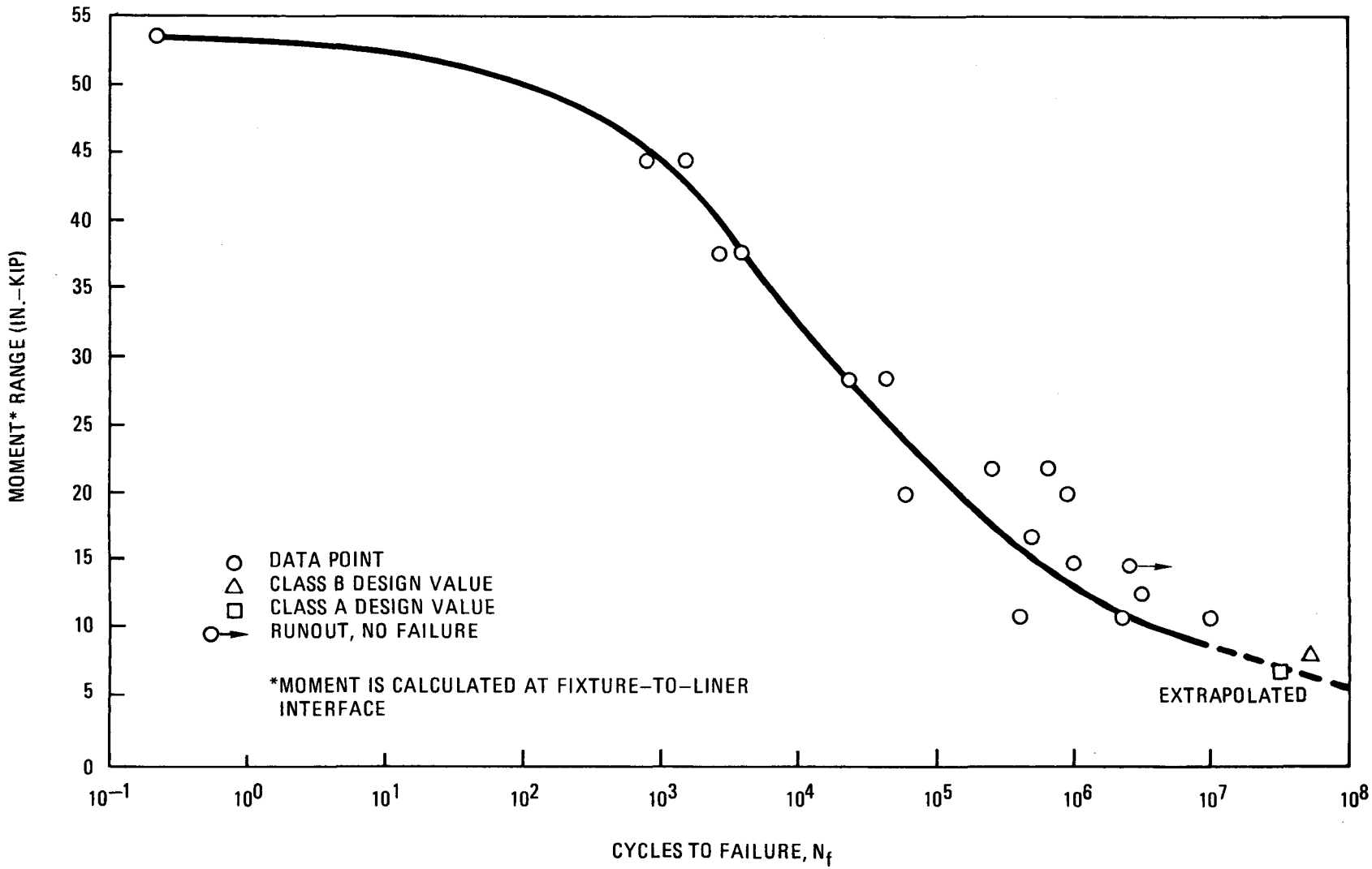

Fig. 11. Results of transverse input CAF cyclic failure tests

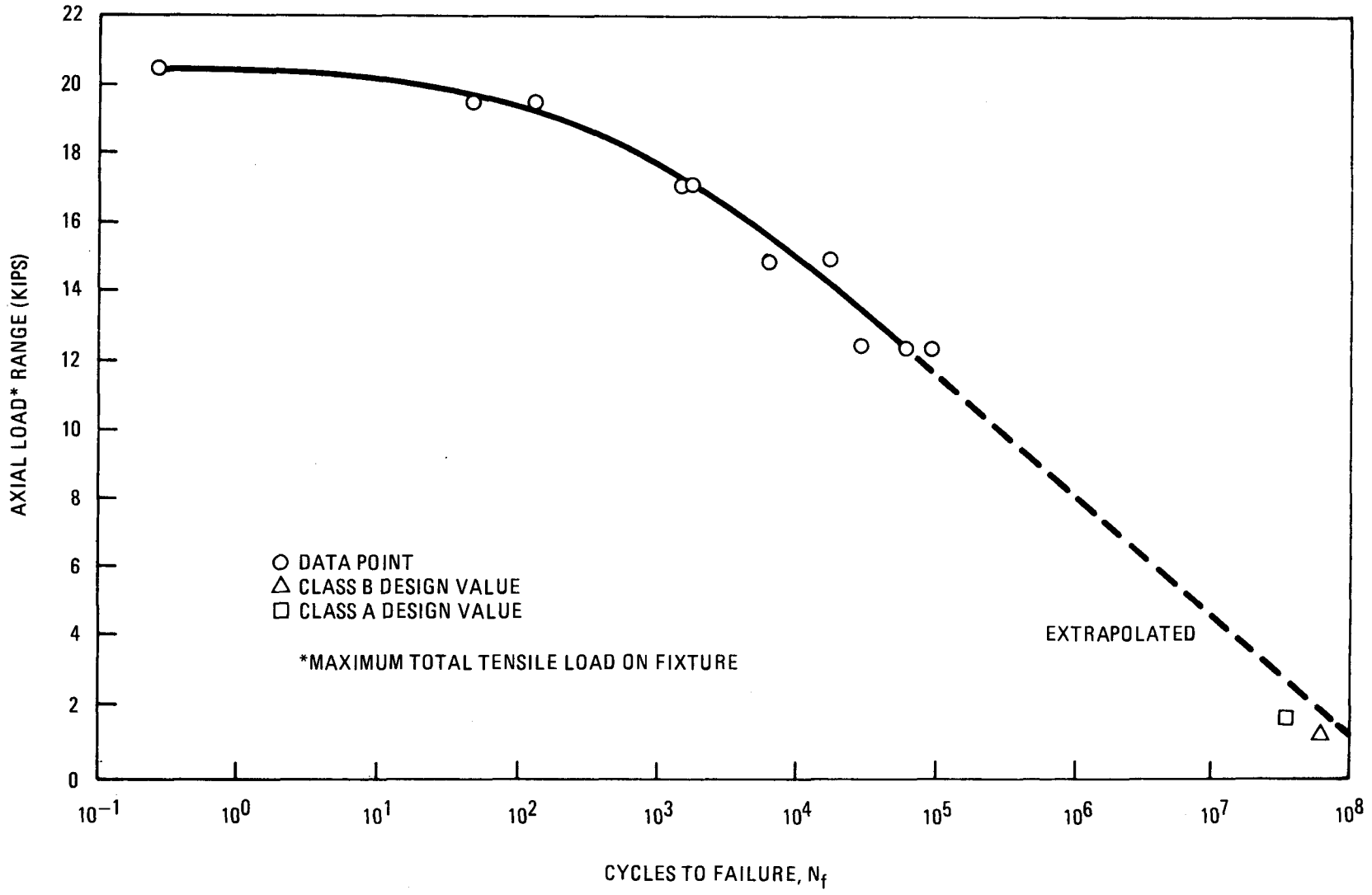

Fig. 12. Results of axial input MER cyclic failure tests

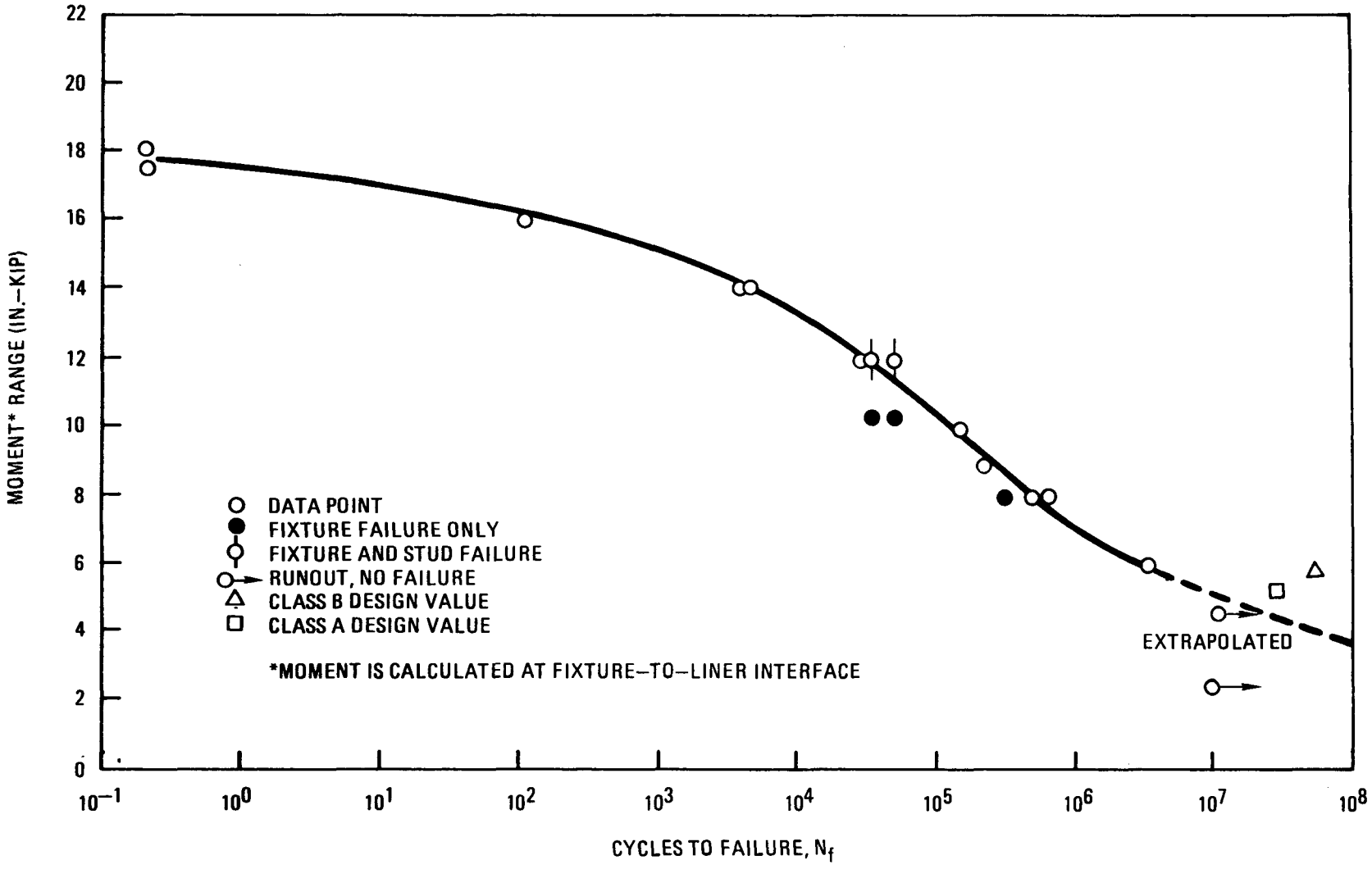

Fig. 13. Results of transverse input MER cyclic failure tests

9. DISCUSSION

9.1. GENERAL

The two most significant influences on the welded studs with respect to their ability to meet fatigue life requirements in the HTGR environment are as follows: (1) the chatter, or stick-slip, phenomenon, which is postulated to produce a marked increase in stud stress cycles compared with reactor operational thermal cycles, and (2) the complex superposition of stud stresses resulting from elastic deformation of the beveled flange surface of the CAF and MER.

The chatter phenomenon is discussed in Section 9.2 and the stress superposition is discussed in Section 9.3. The failures in the CAF and MER are discussed in Section 9.4.

Metallurgical analysis of a sample of the failed studs was performed using scanning electron microscopy (SEM) and optical metallography methods. The results of these analyses are given in Section 9.5.

9.2. CHATTER

Chatter, or stick-slip, is a well-documented phenomenon (Refs. 4,5, and 6). Its occurrence is based on the fact that the coefficient of dynamic friction between two surfaces sliding with respect to each other is less than the coefficient of static friction between the same two surfaces when motion is impending.

In the HTGR thermal barrier design, the surfaces sliding with respect to each other are the cover plates and the MER washers (see Fig. 2). The driving force is provided by thermal expansion and contraction of the cover plates due to reactor thermal cycling.

A simplified explanation of the transverse mode of chatter is as follows. The cover plate is assumed to be fixed at its center by the CAF and to expand outward toward the MER as reactor temperature increases. The adjacent cover plate is assumed to be absent. This is a conservative method of accounting for asymmetries such as varying friction coefficients, manufacturing irregularities, uneven cover plate temperature distributions, and non-symmetrical placement of attachment fixtures to accommodate thermal barrier penetrations. As the cover plate expands, relative motion tends to occur at the washer interface. This motion is resisted by the static friction force $\mu_s N$ (where μ_s is the static friction coefficient and N is the normal force). As the cover plate expansion force builds up, it is stored as strain energy in the plate and in the MER and its attachment studs.

When the expansive or driving force exceeds the resisting or static friction force, slipping occurs at the interface. Motion during the slip is controlled by the dynamic friction coefficient, inertia of the MER, and the stored strain energy. The strain energy stored in the MER, its inertia, and the lower friction coefficient cause it to spring back to a position beyond its initial position. As the cover plate continues to expand, the MER is returned to its initial position, then deflected beyond this position as the static friction force builds and the cycle is repeated. Each deflection and spring-back cycle is translated into a low-magnitude stress cycle in the studs. The theory also applies as the cover plate cools and contracts.

Curved thermal barrier cover plates give rise to axial chattering loads by the same type of mechanism (Ref. 8).

Quantitative values for the number of stick-slip cycles per reactor thermal cycle (the chatter multiplier) depend upon the values of the following parameters: the mass and stiffness of the parts, the normal force between the sliding surfaces, the purity level of the helium environment, the temperature and rate of temperature increase, the static and dynamic friction coefficients, and the damping present in the system.

A conservative analysis using the single degree of freedom system described above (single cover plate fixed at center and single MER) indicates that the chatter multiplier may be as high as 3660. That is, 3660 chatter cycles may occur for each reactor thermal cycle, resulting in a total of 8.2×10^7 or nearly 10^8 chatter cycles over reactor design life. The predicted number will vary with reactor location and thermal cycle due to variation of one or more of the parameters used in the analysis.

9.3. SUPERPOSITION OF STUD STRESSES

Figure 2 indicates the gap between the lower surface of a typical thermal barrier attachment fixture and the PCRV liner due to the beveled lower surface of the attachment fixture. The bevel was designed on the basis of one flange configuration fitting all surface curvatures within the PCRV cavity to which both Class A and Class B thermal barriers are applied. For the smallest radius of curvature, the CAF and MER would fit nearly flush. For the largest radius of curvature, the gap at the outer edges would be the largest. This test program was run with flat plates simulating the largest radius condition. Figure 9 shows that studs No. 1 and No. 3 are located in the "non-contacting" area of the flange. As the lock nuts on studs No. 1 and No. 3 were tightened, pre-loading the studs, the flange tended to flex, inducing large bending stresses in the studs as well as in the flange. The stud bending stresses were superimposed on the axial pre-load stresses. These steady-state stresses were then superimposed on the alternating stress history.

In order to graphically illustrate the effect of the steady-state stresses in reducing the allowable alternating stress for a given number of cycles, a Soderberg diagram is presented (Fig. 14). This diagram is similar to the well-known Goodman diagram with the additional criterion that the total stress must be less than the stress at 0.2% elongation. It clearly shows that as the steady-state stress increases, the allowable alternating stress decreases for the same number of cycles.

9.4. ATTACHMENT FIXTURE FAILURES

Class A MERs exhibited fatigue cracks in the external threads of the cylindrical section. These cracks appeared during transverse loading. Failure occurred in the intermediate to high cycle fatigue range. The failure occurred at a clearly defined stress riser which has been eliminated by subsequent redesign.

Class B MERs exhibited fatigue cracks in the base of the spot face at the intersection of the cylindrical section and the base flange. Failure occurred during transverse loading in the high cycle range. The failure occurred at a clearly defined stress riser which has subsequently been eliminated.

The design changes specified in Section 4 provide an overall reduction in stress levels by employing larger section values, as well as eliminating stress risers.

Class B CAFs failed by separation of the cylindrical section from the base flange under an axial ultimate load test. Metallurgical analysis revealed that this part had a very large grain structure. The Class B CAFs satisfactorily produced stud failures under transverse loading. Class A (carbon steel) CAFs were substituted for the Class B (Hastelloy X) CAFs in the axial tests to complete the program. The use of cast Hastelloy X has been suspended.

9.5. METALLURGICAL EXAMINATION

The failure data for the transversely loaded 1/2-in. studs exhibited the widest range of scatter. Consequently, five failed studs were selected for failure mode evaluation to determine whether or not metallurgical factors had contributed to the data scatter. All five specimens were from the No. 1 stud location, which is the location of the most highly stressed stud under transverse loading. The studs were selected from tests which had produced a wide range of failure data scatter (tests No. 13, 16, 7, 8, and

59). The evaluation included the use of scanning electron microscopy and optical metallography. All five stud specimens failed in the thread area. The failure mode was common to all specimens. That is, the fatigue crack appears to have initiated at the root of the thread in the inner part of each stud with respect to the fixture post (the 11 o'clock position of stud No. 1, Fig. 9) and to have grown outwardly until rupture by shear at the outer region of the stud.

Figure 15 shows the fatigue area. The area of shear rupture which occurred at the end of the test is shown in Fig. 16. The microstructures of the cross-sectional areas perpendicular to the fracture surface areas are shown in Fig. 17. Figure 17(a) shows the microstructure of the cross-sectional area at the fatigue initiation site. The deformation structure resulting from the thread forming operation is clearly shown in the figure. Figures 17(b) and 17(c) show typical structures of the cross-sectional areas perpendicular to the fatigue area and the shear rupture area, respectively. Figure 17(c) clearly shows the plastic deformation resulting from shear rupture.

The microstructure of an untested 1/2-in. stud was examined by optical metallography. Special emphasis was placed on the thread area during the course of examination in an attempt to correlate the scatter of data with possible defects in the stud at the thread area. The typical structures at both the crest and root in the thread area are shown in Fig. 18, which reveals a surface layer of plastic deformation resulting from the forming operation of the thread.

Based on the examination, metallurgical factors were not believed to contribute to the relatively large scatter of the data obtained in the transverse load tests of the 1/2-in. studs.

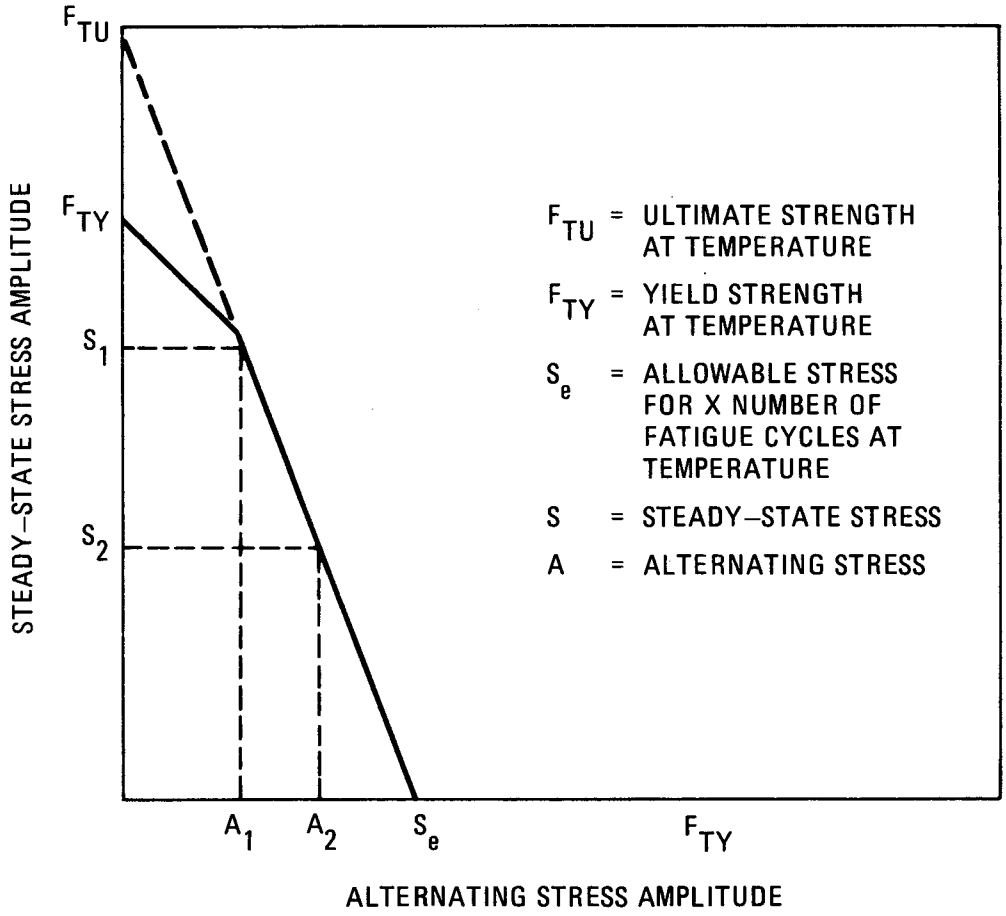

Fig. 14. Soderberg diagram showing reciprocal relationship between the steady-state and alternating stress amplitudes

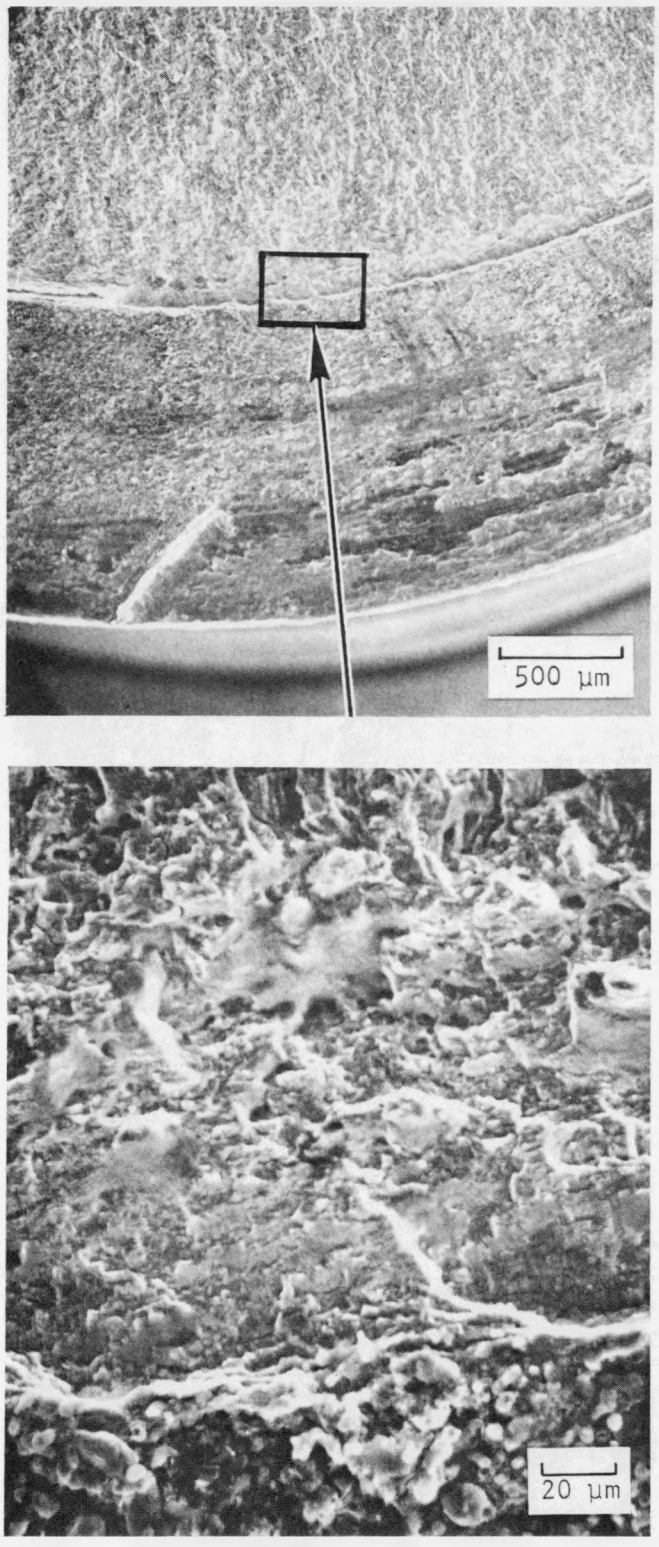

(a)

(b)

Fig. 15. SEM photomicrographs showing the stud specimen surface believed to be the fatigue initiation site. (a) is at low magnification. The curved line represents the thread root. (b) shows the area enclosed by the rectangle at high magnification.

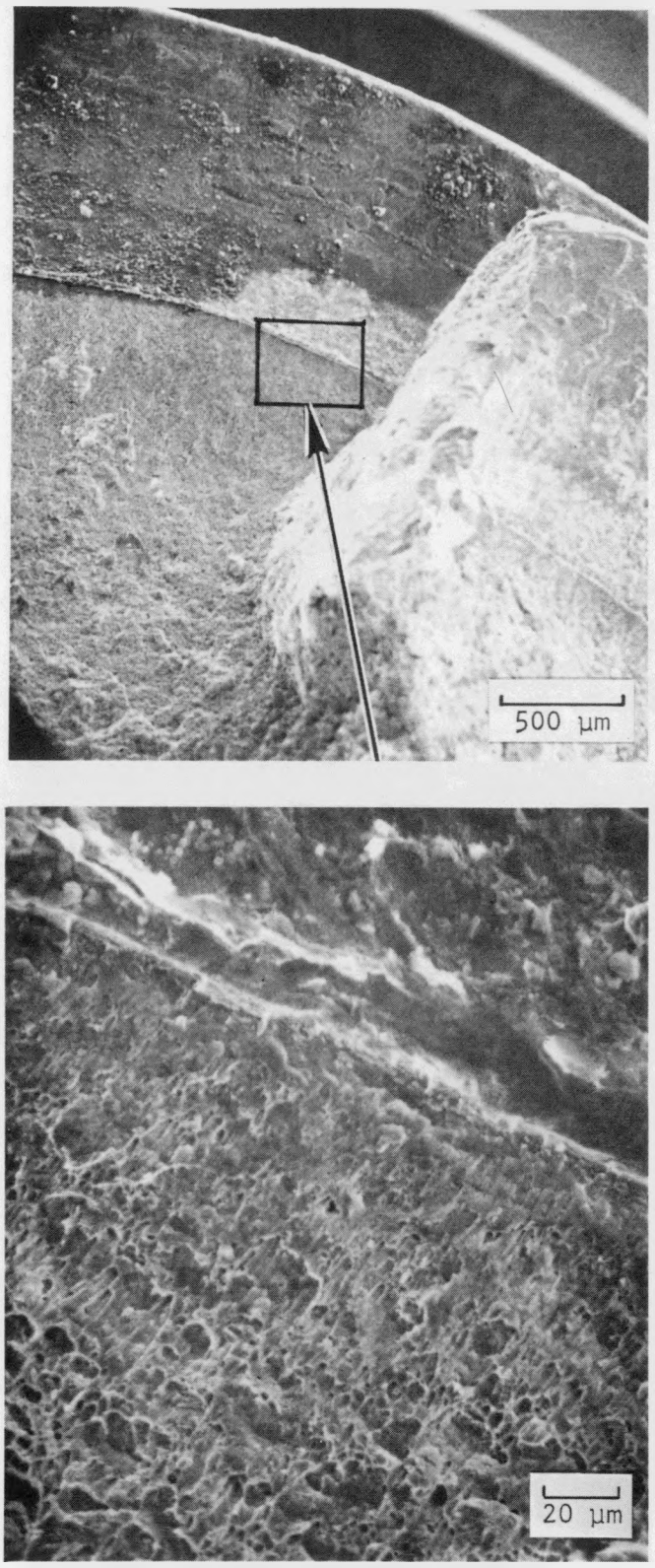

(a)

(b)

Fig. 16. SEM photomicrographs showing the shear rupture area of the stud specimen. (a) is at low magnification, and (b) shows the area enclosed by the rectangle at high magnification. Note the dimple rupture, which is a typical shear rupture.

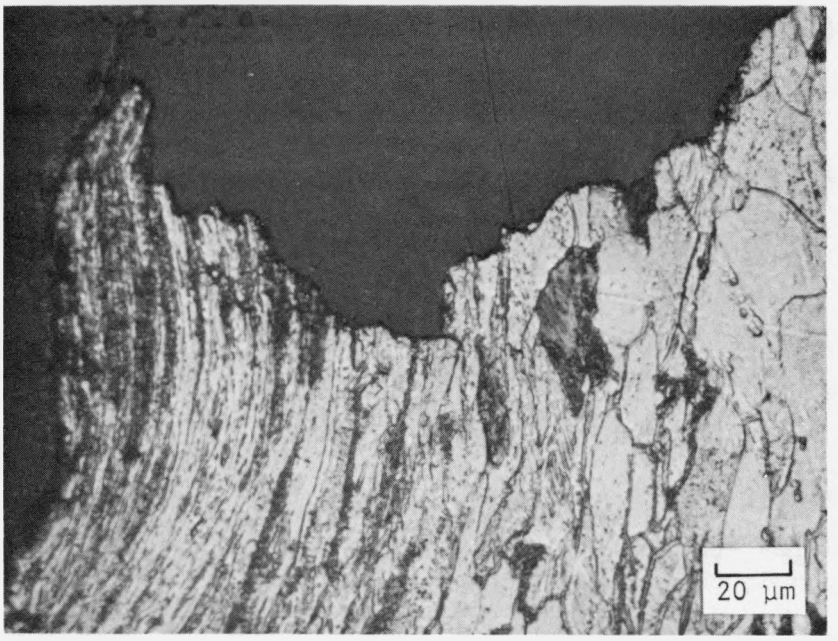

Fig. 17(a). Microstructure of cross-sectional area perpendicular to fatigue initiation site in the specimen

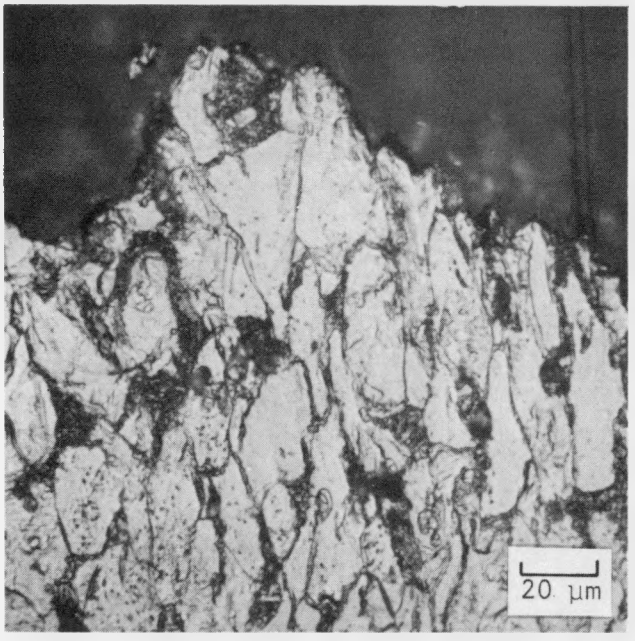

Fig. 17(b). Microstructure of cross-sectional area perpendicular to fatigue area in the specimen

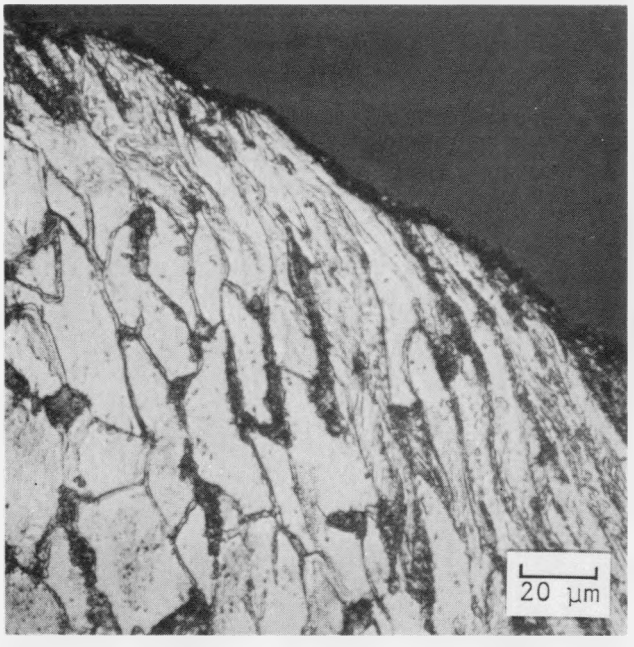

Fig. 17(c). Microstructure of cross-sectional area perpendicular to shear rupture area in the specimen

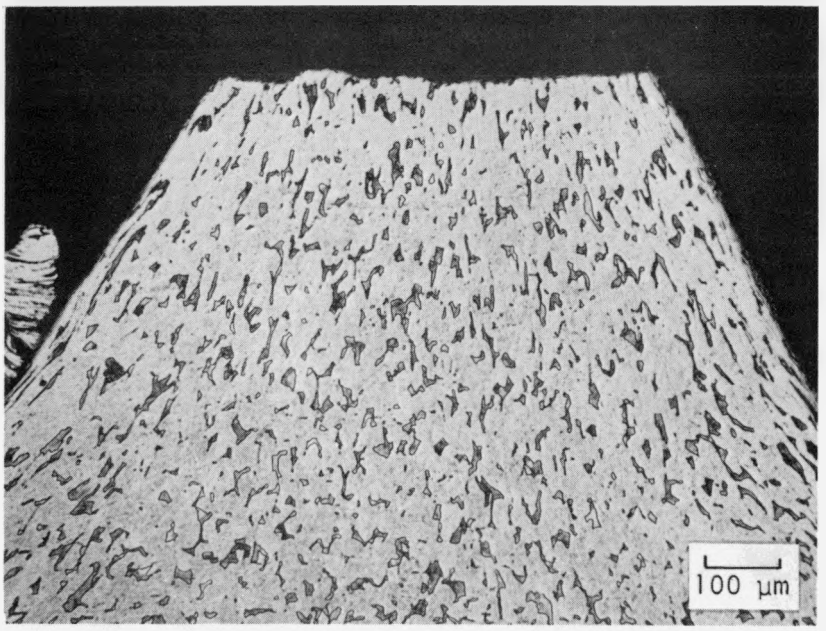

(a)

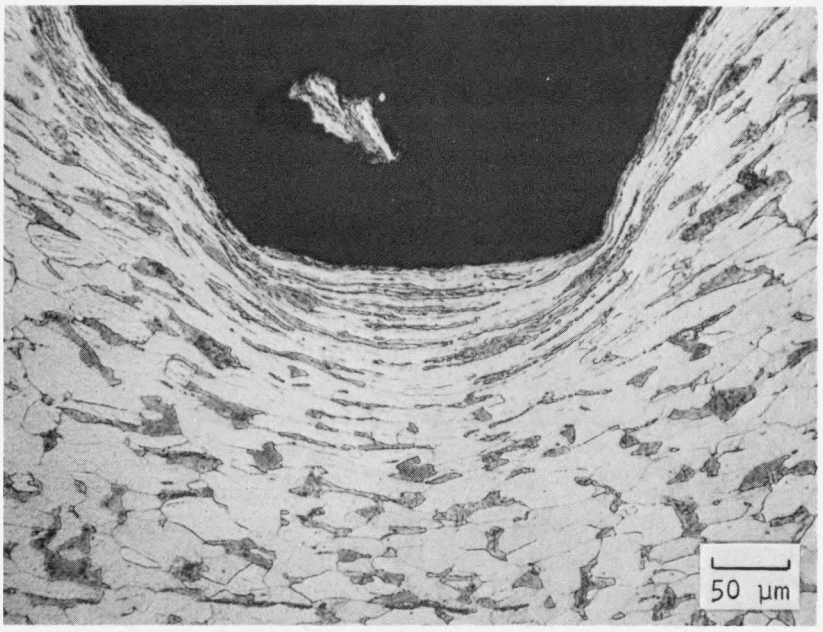

(b)

Fig. 18. Typical microstructures at (a) the crest and (b) the root in the thread area for an untested 1/2-in. stud

10. REFERENCES

1. "Specification for DV&S Thermal Barrier Chatter Test," General Atomic Company, unpublished data.
2. "ASME Boiler and Pressure Vessel Code," Case 1592-7, Para. 3213.8 and 3213.9, American Society of Mechanical Engineers, New York.
3. Derjaguin, B. V., V. E. Push, and D. M. Tolstoi, "A Theory of Stick-Slip Sliding of Solids," in Proceedings of the Conference on Lubrication and Wear, London, October 1-3, 1957, The Institute of Mechanical Engineers.
4. Dokos, S. J., "Sliding Friction Under Extreme Pressure," J. Appl. Mech. 13A, 148-156 (1946).
5. Voorhes, W. G., "Investigation of Stick-Slip in Simulated Slideways," Lubrication Eng., 457-462 (Nov. 1963).
6. "Design Criteria: Representative Plant Transients," Table II, page 23, General Atomic Company, unpublished data.
7. "Specification for Thermal Barrier Stud Welding and Inspection," General Atomic Company, unpublished data.
8. Wonacott, G., "Thermal Barrier Attachment Fixture Lower Base Structural Evaluation," General Atomic Company, unpublished data.